Relaxation in ZnSe:Cr^{2+} investigated with longitudinal ultrasonic waves

V. V. Gudkov,* A. T. Lonchakov,† V. I. Sokolov,‡ and I. V. Zhevstovskikh§
Institute for Metal Physics, Ural Department, Russian Academy of Sciences, Ekaterinburg, Russia
(Received 15 September 2005; revised manuscript received 30 November 2005; published 25 January 2006)

Temperature dependences of phase velocity and absorption of ultrasound were investigated in ZnSe crystal doped with Cr^{2+} ions at the frequencies 32–158 MHz. Absorption peak and variation of phase velocity found in the temperature interval 10–20 K were interpreted as manifestation of the Jahn-Teller effect. Temperature dependences of relaxation time, relaxed, and unrelaxed moduli $C=\frac{1}{2}(C_{11}+C_{12}+2C_{44})$ were restored. The dependences were compared with the results of such investigations in ZnSe:Ni^{2+} and analyzed regarding lattice stability of the crystals. Fitting of the temperature dependence of the relaxation time was done with account of thermal activation over the potential barrier, quantum tunnelling with phonon emission, and two phonon process analogous to Raman scattering. Thermal activation proved to be the dominant mechanism of relaxation above 6 K and quantum tunnelling—below this temperature.

DOI: 10.1103/PhysRevB.73.035213 PACS number(s): 61.72.Vv, 43.35.+d

I. INTRODUCTION

The physical properties of binary zinc-blende semiconductors conditioned by their electronic band structure are investigated by many authors (see, for example, Refs. 1 and 2, and references therein). Particular attention was paid to the crystals with $3d$ impurities[3–5] because of their possible application in spintronic devices[6] and optoelectronics.[7]

Our former study of a representative of such materials has been initiated by anomalies in heat conductivity found in ZnSe crystals doped with iron[8] and nickel.[9] We have investigated ZnSe:Ni^{2+} crystal with the use of neutron diffraction and ultrasonic method.[10] The concentration of the dopand has been $\approx 10^{20}$ cm^{-3}. Distortion of the (400) Bragg reflex shape observed at the temperature $T=13$ and 4.2 K with respect to the Gaussian form at 60 K has been interpreted as the result of phase transition. Ultrasonic absorption α and phase velocity v have been measured with the use of longitudinal waves generated at 52 and 154 MHz and propagated along the $\langle 110\rangle$ crystallographic axis. The experiments have revealed softening of the effective elastic modulus below 50 K and peak of absorption at ≈ 15 K. Such anomalies have not been observed in a pure ZnSe crystal and have been interpreted as ones caused by the dopand. Further ultrasonic investigations[11] carried out with the use of transverse ultrasonic waves propagating along the $\langle 110\rangle$ axis have proved that the peak of absorption and sufficient softening of the appropriate modulus were observed only for the mode, polarized along $\langle 100\rangle$. Data on phase velocities of all the modes made it possible to restore all the elastic moduli of a cubic crystal, C_{11}, C_{12}, and C_{44}.[12] It has been proved that only the modulus C_{44} exhibited the softening. This fact has indicated the type of deformations coupled with the order parameter (namely, ε_4). Similar character of softening has been reported in Yb_4As_3 (Ref. 13) and conclusion has been done about trigonal symmetry of the low temperature phase. Following this approach we can state that the low temperature structure of ZnSe:Ni^{2+} also could be a trigonal one. The Jahn-Teller effect has been proposed as a possible reason of the phase transition since (i) this effect has been observed in such crystal before,[14] (ii) similar peak of ultrasonic absorption, interpreted as due this effect, has been found in Al_2O_3:Ni^{3+} (see, review[15]), and (iii) this effect manifests itself as at least local deformations of the crystal near the impurity and result in lattice instability. In our case the instability has the form of softening the elastic modulus C_{44}. If to do some assumptions, the temperature dependence of ultrasonic absorption can be described in analytical form and appropriate fitting may give useful information about the physical parameters of the investigated crystal, particularly, about its dopand's electron system. Namely, the relaxation time τ, the energy of the lowest state splitting, the height of the barrier between potential minima, corresponding to different directions of distortion, and some other. Notice that the dependence $\tau(T)$ can point out the mechanism of relaxation and, as well, can be used to restore the temperature dependences of the elastic molduli: unrelaxed (adiabatic) C^U and relaxed (isothermal) C^R. When experimental results are compared with theoretical calculations, these moduli may be even more important than the dynamic ones C (i.e., measured in an experiment at a certain frequency ω), because it is the isothermal or adiabatic moduli that enter in the expressions for free energy and other thermodynamic potentials. The procedure of $C^U(T)$ and $C^R(T)$ restoring has been developed and applied for ZnSe:Ni.[16] Different temperature dependences have been revealed: softening of both $C^U(T)$ and $C^U(T)$ below 50 K and temperature independence of $C^U(T)$ below ≈ 10 K. In addition, a linear part of both the curves has been noticed in the interval $9<T<21$ K. Change in the character of the curves at $T=21$ K has been suggested as indication of the phase transition point.

Notice that the developed procedure is quite new. It requires quantitative data on both $\alpha(T)$ and $v(T)$. Moreover, the frequency of ultrasonic wave should be high enough to provide the condition $\omega\tau(T)=1$ in the region of available temperatures.

In the experiments reported here we have tried to apply this new procedure to another object—zinc selenide doped with Cr. The Jahn-Teller effect in ZnSe:Cr^{2+} has been found in spin resonance experiment[17] and investigated in emission and absorption spectra.[18] As well as in ZnSe:Ni^{2+}, heat con-

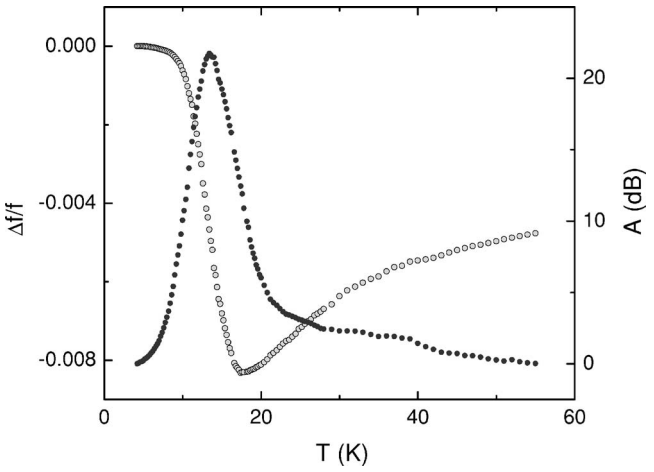

FIG. 1. Temperature dependences of $[f(T)-f(4.2)]/f(4.2)$ (open circles) and attenuation of ultrasound (filled circles), respectively, the level at $T=4.2$ K measured at 54.4 MHz. Ultrasound passage $\ell=0.717$ cm.

ductivity have shown deep minimum in temperature dependence at low temperature in this crystal.[19] The ground term of Cr^{2+} in tetrahedral coordination is ${}^5T_2$ instead of ${}^3T_1$ for Ni^{2+}. Thus, we expected to find even more pronounced anomalies in $\alpha(T)$ and $v(T)$.

II. EXPERIMENT

A. Experimental details and initial data

Two specimens were cut of the single crystal with concentration of the dopand $N=10^{20}$ cm^{-3}. The concentration was measured with the use of optical emission spectroscopy of inductively coupled plasma. The specimens had the form of a cylinder with distances between the parallel faces $L_1=2.39$ and $L_2=4.95$ mm.

Ultrasonic investigations were carried out using a pulse setup operating as a variable-frequency bridge (see pp. 25–30 in Ref. 20). Longitudinal waves propagated along the $\langle 110\rangle$ crystallographic axis. They were generated and registered by $LiNbO_3$ piezoelectric transducers in the frequency interval 32–158 MHz. Radio-pulse duration τ_p was about 1 μs and was less than the double passage time of ultrasound from one face of the specimen to another. In this technique the relative change of the frequency f, corresponding to the bridge balances obtained at T and T_0, is determined by phase velocity of ultrasonic mode and the distance of the wave passage ℓ as follows:

$$\frac{\Delta f}{f_0}=\frac{\Delta v}{v_0}-\frac{\Delta \ell}{\ell_0}, \tag{1}$$

where $f_0=f(T_0)$, $v_0=v(T_0)$, and $\ell_0=\ell(T_0)$, $\Delta f=f(T)-f_0$, $\Delta v=v(T)-v_0$, $\Delta \ell=\ell(T)-\ell_0$. Temperature variation of the specimen dimension was neglected and, therefore, we omitted the last term in Eq. (1) in processing of the experimental results.

The data obtained at the frequency 54.4 MHz and $\ell=3L_1$ are given in Fig. 1. If we take into consideration the accuracy of our measurements ($\approx 10^{-6}$ in $\Delta f/f$ and ≈ 0.02 dB in attenuation A), one can notice that variations of the measured parameters are very large.

B. Ultrasonic absorption and dispersion

Effective dynamic modulus C determines the phase velocity of a certain normal mode propagating along a certain crystallographic direction as follows:

$$C=\rho v^2, \tag{2}$$

where ρ is the material's density. The term "effective" means that it is a linear combination of the moduli defined in the coordinate system of the principal axes of a cubic crystal and "dynamic" means that it is frequency dependent. In our experiment we used a longitudinal wave propagating along [110]. Omitting (only in the following expression) the superscripts U or R, we remind the form of the discussed effective moduli (dynamic, unrelaxed, and relaxed):

$$C=\tfrac{1}{2}(C_{11}+C_{12}+2C_{44}). \tag{3}$$

We will use the time and spatial dependences of the variables as $\exp[i(\omega t-\mathbf{kr})]$. Attenuation of the wave can be described with the help of the imaginary part of the frequency or of the wave number. We will choose the last variant. In this case a well-known definition written for real numbers $k=\omega/v=\omega/\sqrt{C/\rho}$ is replaced with $k=(\omega/v)-i\alpha=\omega/\sqrt{C/\rho}$ in which k and C are defined as complex numbers. If attenuation $\alpha \ll \omega/v$ (it is the definition of a weakly damping wave) and $\Delta v=v(T)-v_0 \ll v_0$ we have

$$\alpha=\frac{1}{2}\,\mathrm{Re}\,k\frac{\mathrm{Im}\,C}{\mathrm{Re}\,C(T_0)},\quad \frac{\Delta v}{v_0}=\frac{1}{2}\frac{\mathrm{Re}\,\Delta C}{\mathrm{Re}\,C(T_0)}. \tag{4}$$

Remind, in this expression and in all others below we accept k and C as complex variables. The expression for k shows that α characterizes the attenuation of amplitude, not energy. It is useful to present the data on absorption and dispersion of a wave in the form of Re k and Im k. In this case they have common units (cm^{-1}) and it is possible to show the dependences in the same coordinates.

The data presented in this form as a function of inverse temperature are given in Fig. 2. The reason for this presentation is the dependences as functions of inverse temperature will be clear when we discuss the temperature dependence of the relaxation time. The values $\mathrm{Re}[k(T^{-1}\to\infty)]$ and $\mathrm{Im}[k(T^{-1}\to\infty)]$ were taken as extrapolation of the curves $\mathrm{Re}[k(T)]$ and $\mathrm{Im}[k(T)]$ to $T=0$ K. Thus, in our further consideration $T_0=0$ K. Remind, $-\mathrm{Im}\,\Delta k$, measured in cm^{-1} is the equivalent of $\Delta\alpha$, measured in nepers/cm. Therefore, the vertical axis shows negative values to present peak of absorption as maximum of the curve.

Notice a remarkable feature of the curves: maximum of $-\mathrm{Im}\,\Delta k$ corresponds to the temperature, at which $-\mathrm{Re}\,\Delta k$ reaches a half of its maximum value. It is typical for a phenomenon of relaxation nature.

C. Relaxation time and elastic moduli

A description of a relaxation-origin phenomenon in an ultrasonic wave propagation can be done with the use of the

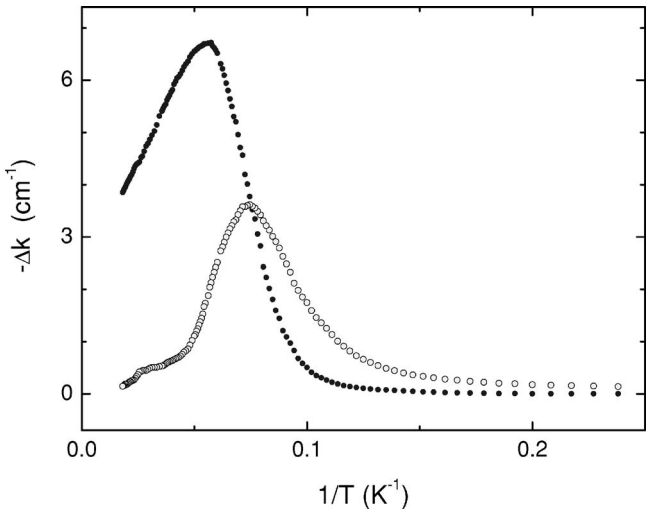

FIG. 2. Real (filled circles) and imaginary (open circles) components of the complex wave number versus inverse temperature obtained at 54.4 MHz. $\Delta k = k(T^{-1}) - k(\infty)$.

Zener equation. Following the approach given in Ref. 21 we will write this equation in the form

$$\varepsilon + \tau \frac{d\varepsilon}{dt} = \frac{\sigma}{C^R} + \frac{\tau}{C^U}\frac{d\sigma}{dt}, \tag{5}$$

where ε is elastic strain, σ is stress, and τ is relaxation time. We will assume small difference between relaxed and unrelaxed compliance, $1/C^R - 1/C^U \ll 1/C^R, 1/C^U$. In this case solution of Eq. (5) gives an expression for dynamic modulus,

$$C = C^U - \frac{C^U - C^R}{1+\omega^2\tau^2}(1 - i\omega\tau) = C^R + \frac{C^U - C^R}{1+\omega^2\tau^2}(\omega^2\tau^2 + i\omega\tau). \tag{6}$$

It is clear, that C^U and C^R represent the limits of C as function of $\omega\tau$: $C^U = C(\infty)$ and $C^R = C(0)$. If there would be no other mechanisms of energy loss, the moduli would be adiabatic C^S and isothermal C^T ones, respectively.

The expression for ultrasonic absorption, deduced from Eqs. (4) and (6), has the form

$$\alpha = \frac{1}{2v}\frac{C^U - C^R}{\mathrm{Re}\, C}\frac{\omega^2\tau}{1+\omega^2\tau^2} = \frac{1}{2}\,\mathrm{Re}\, k \frac{C^U - C^R}{\mathrm{Re}\, C}\frac{\omega\tau}{1+\omega^2\tau^2}. \tag{7}$$

Notice that Eq. (7) represents the relaxation-origin contribution to the total absorption. At low temperatures this mechanism can be the principal one. Thus, it is possible to assume $\alpha(0) = 0$, $C(0) = \mathrm{Re}\, C(0) \equiv C_0$, $k(0) = \mathrm{Re}\, k(0) \equiv k_0$, and the temperature variations of Re C and Im C are small, respectively, C_0. In view of these assumptions we can simplify the form of Eq. (7) and present it as

$$\alpha = \frac{k_0}{2}\frac{C^U - C^R}{C_0}\frac{\omega\tau}{1+\omega^2\tau^2}. \tag{8}$$

Now we must do some propositions about mechanism of relaxation. Ultrasonic wave produces the elastic distortions of the crystalline lattice. These distortions change slightly the system of energy levels of the impurity $3d$ electrons. The new system is time dependent and characteristic time of its alternation is the wave's period $2\pi/\omega$. Perturbation of the initial temperature-equilibrium system leads to a nonequilibrium distribution of the electrons. This distribution should relax with a characteristic time τ. The energy of the electronic system is transmitted during the relaxation process into the thermal energy of the lattice leading to absorption of the wave.

We propose that we observe relaxation in the $3d$ electron system formed with account of Jahn-Teller coupling and follow the approach[15] used for processing the data of ultrasonic experiment in Al_2O_3:Ni^{3+}. It is a cubic crystal with the Jahn-Teller ion in octahedral crystal field. The ion's ground state is triply degenerate. The energy minima corresponding to different direction of the lattice distortion are separated by the potential barrier V_0. Quantum tunnelling leads to splitting the ground state into a doublet (E state) and a singlet (A state). It was proposed that the crystal has inevitable random strains those lower one energy levels with respect to the others and relaxation occur in the system of these new energy levels distorted by the ultrasonic wave.

In our experiment the matrix (see band structure of ZnSe in Ref. 22) and the impurity are not identical to those discussed above. The principal difference is that the impurity has tetrahedral coordination in ZnSe and, as a result, another set of vibronic normal modes. However, (i) the ion's ground state is triply degenerate as well, (ii) according to Ref. 15, the Jahn-Teller coupling to ϵ distortions in tetrahedral complex is, in principle, identical to that of ε_g distortions of octahedron, and (iii) although the coupling to τ_2 distortions is more complicated in ZnSe:Cr^{2+}, qualitatively it is the same.

Thus, we use the following expression for the relaxation rate:

$$\tau^{-1} = \tau_T^{-1} + \tau_t^{-1} + \tau_R^{-1}, \tag{9}$$

where τ_T^{-1} describes thermal activation over the barrier, τ_t^{-1}, tunnelling accompanied by phonon emission; and τ_R^{-1}, two phonon process analogous to Raman scattering. They are given by

$$\tau_T^{-1} = 2\nu_0 e^{-V_0/\kappa T}, \tag{10}$$

$$\tau_t^{-1} = \frac{6\Gamma^2\beta^2}{\pi\rho\hbar^4 v_0^5}\frac{u_0}{\kappa T}\frac{2 + e^{-u_0/\kappa T}}{(1 - e^{-u_0/\kappa T})}, \tag{11}$$

$$\tau_R^{-1} = \frac{9\Gamma^2\beta^4(\kappa T)^3}{\pi\rho^2\hbar^7 v_0^{10}}, \tag{12}$$

where κ is Boltzmann constant, ν_0 is vibrational frequency in a potential well, 3Γ is energy separation between the Jahn-Teller A and E states, 3β is splitting of the states per unit strain (appropriate component of deformation potential tensor), and u_0 is the averaged energy, characterizing local minimum of the Jahn-Teller states caused by random strains in the crystal. Contribution of the two-phonon process was considered in Ref. 15 as negligible but it was mentioned that in crystals with lower Debye temperature it might be important. The Debye temperature of Al_2O_3 is 1048 K while in ZnSe it

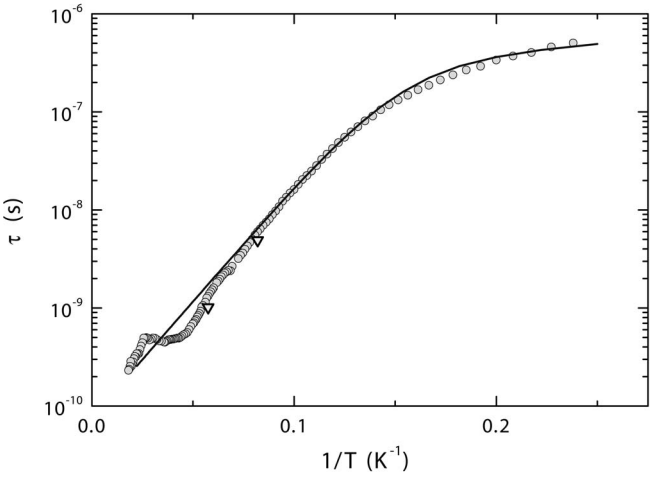

FIG. 3. Relaxation time versus inverse temperature. Circles represent experimental data obtained at fixed frequency $\omega/2\pi = 54.4$ MHz and processed with Eq. (16), triangles represent the maxima of absorption obtained at 32.5 and 157 MHz, solid curve represents the result of fitting done on the basis of Eqs. (9)–(12).

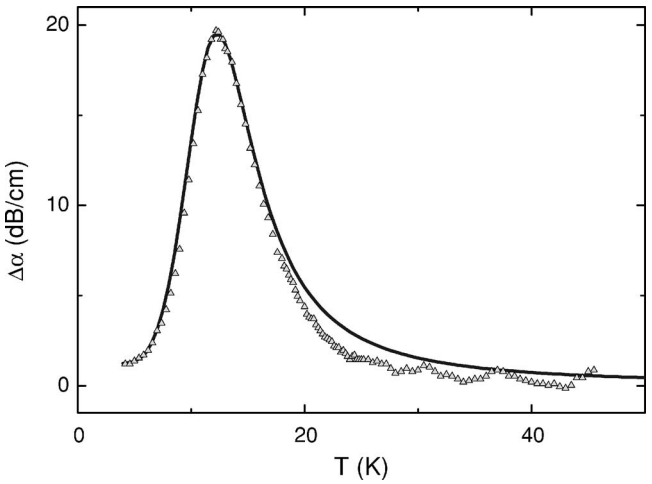

FIG. 4. Temperature dependences of ultrasonic absorption. Triangles represent dependence measured at 32.5 MHz, solid curve represents dependence calculated for 32.5 MHz using the data on $\tau(T)$ and ϵ obtained at 54.4 MHz.

is 279 K. Thus, we will account for all the terms presented in Eq. (9).

The expression for ultrasonic absorption is given by

$$\alpha = k_0 \frac{2N\beta^2}{C_0 \kappa T} f\left(\frac{u_0}{\kappa T}\right) \frac{\omega\tau}{1+\omega^2\tau^2}, \tag{13}$$

where $f(u_0/\kappa T)$ is a smooth function with the limit $f(0)=1$. Using this limit we can write

$$\alpha = k_0 \frac{\epsilon}{\kappa T} \frac{\omega\tau}{1+\omega^2\tau^2}, \tag{14}$$

where

$$\epsilon = \frac{2\alpha_m \kappa T_m v_0}{\omega}, \tag{15}$$

is the constant with dimension of energy, α_m is the maximum value of absorption and T_m is the temperature, at which it is observed. Notice that all the parameters on the right-hand part of Eq. (14), except τ, are temperature independent.

In fact we replaced $(C^U - C^R)/C_0$ in Eq. (13) by a function $\propto 1/T$. Thus, *the method described below can be applied not only to the Jahn-Teller effect but to all the phenomena of relaxation nature, those permit such substitution*.

Equation (14) makes it possible to express τ as function of T, α, and ω. Moreover, taking in account that maximum $\alpha(T)$ is achieved at $\omega\tau=1$, we can write the expression in terms of the parameters measured in the experiment,

$$\tau = \frac{1}{\omega}\left(\frac{\alpha_m T_m}{\alpha T} \pm \sqrt{\frac{\alpha_m^2 T_m^2}{\alpha^2 T^2} - 1}\right). \tag{16}$$

Solutions correct from a physical point of view are provided by sign "+" before the square root at $T < T_m$ and sign "−" at $T > T_m$. The result of application for this equation to our data at 54.4 MHz is presented in Fig. 3. Remind, the curve was obtained using the major assumption of $(C^U - C^R)/C_0 \propto T^{-1}$.

Free of this assumption the method is based on the condition that the absorption maximum occurs at $\omega\tau(T) \approx 1$. Experiments carried out at a number of frequencies are required in this case. To check the mentioned assumption at least in a restricted interval of T, we have measured the dependence $\alpha(T)$ at 32.5 and 157 MHz. The results of these measurements are also shown in Fig. 3. One can see that both the methods give similar magnitudes of τ.

To decide, whether the Eq. (9) describes the measured dependence $\tau(T)$ correctly or not, we completed fitting and presented its result with a solid line in Fig. 3. The parameters used in the fitting were $\beta = 10^4$ cm^{-1}, $\Gamma = 0.019$ cm^{-1}, $\nu_0 = 6.5$ GHz, $u_0 = 0.1$ cm^{-1}, $V_0 = 38$ cm^{-1}, $C_0 = \rho v_0^2$, $\rho = 5.42$ g/cm^3, and $v_0 = 4.22 \times 10^5$ cm/s.

Verifying the validity of our approach we simulated the curve $\alpha(T)$ for 32.5 MHz using the data on the relaxation time measured at another frequency. We substituted $\tau(T)$ in Eq. (14) by the data obtained at 54.4 MHz. The constant ϵ was calculated with the values of α_m, and T_m also measured at 54.4 MHz. The parameters related to 32.5 MHz were k_0 and ω itself. Figure 4 shows the result of this procedure. One can see that we achieved good quantitative agreement with the experimental results below 20 K. Obviously, at higher temperatures at least one more mechanism of ultrasonic absorption has contribution comparable with that discussed above.

After obtaining the dependence $\tau(T)$ we focused attention on the unrelaxed and relaxed moduli. Using Eqs. (6) and (7) we can derive the following expressions:

$$C^U = \mathrm{Re}\, C + 2\frac{\alpha}{\mathrm{Re}\, k}\frac{\mathrm{Re}\, C}{\omega\tau},$$

$$C^R = \mathrm{Re}\, C - 2\frac{\alpha}{\mathrm{Re}\, k}\, \mathrm{Re}\, C\omega\tau, \tag{17}$$

or accounting small variations of the dynamic modulus,

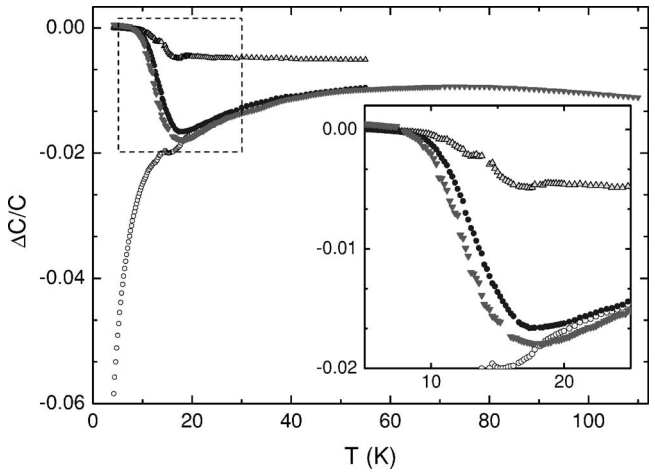

FIG. 5. Temperature dependence of elastic moduli. Filled circles for dynamic modulus $[\mathrm{Re}\, C(T)-C_0]/C_0$, open circles for relaxed modulus $[C^R(T)-C_0]/C_0$, and open triangles for unrelaxed modulus $[C^U(T)-C_0]/C_0$ obtained at 54.4 MHz. Filled triangles for dynamic modulus obtained at 43 MHz. The inset shows the curves in the dashed square.

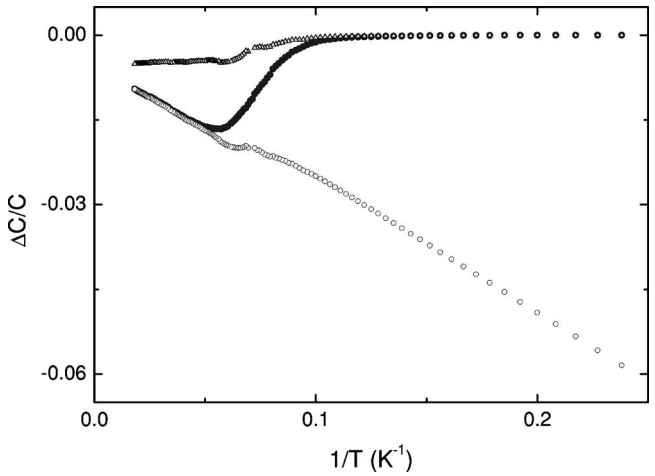

FIG. 6. Elastic moduli versus inverse temperature obtained for 54.4 MHz. Filled circles represent the dynamic modulus $\mathrm{Re}\,\Delta C/C_0$, open circles represent the relaxed modulus $(C^R-C_0)/C_0$, and open triangles represent the unrelaxed modulus $(C^U-C_0)/C_0$.

$$\frac{C^U-C_0}{C_0}=\frac{\mathrm{Re}\,\Delta C}{C_0}+2\frac{\alpha}{k_0}\frac{1}{\omega\tau},$$

$$\frac{C^R-C_0}{C_0}=\frac{\mathrm{Re}\,\Delta C}{C_0}-2\frac{\alpha}{k_0}\omega\tau. \tag{18}$$

Substituting the appropriate variables in Eq. (18) by the experimental data on $\mathrm{Re}\,\Delta C/C_0=2\Delta f/f_0$, τ, and α we obtained the results shown in Fig. 5 along with the temperature dependences of the dynamic modulus measured at 54.4 and 43 MHz. The reason to present the curves obtained at two frequencies was one more chance to check our proposition about relaxation nature of the anomalies. The curves should confirm the following: (i) low temperature and high temperature limits of the dynamic moduli are frequency independent since they represent the unrelaxed and relaxed moduli, respectively, and (ii) transformation from isothermal form of propagation to adiabatic form occurs at lower temperature when the frequency is reduced. These statements do correspond completely to the curves given in Fig. 5.

III. DISCUSSION

The dependences presented in Fig. 5 evidence that the dynamic modulus approximately equals the relaxed one at high temperatures and it becomes close to the unrelaxed modulus below 10 K. At first glance we observe a contradiction: it is well known that the typical process of an acoustic wave propagation has adiabatic form while in our experiment the adiabatic form is established only below 10 K. To understand the reason for this contradiction we should remind that the elastic modulus C in our case may be introduced as the sum of two components, C_B and C_{JT}. The first one represents the main (background) part while the second represents the contribution of the Jahn-Teller effect. The Jahn-Teller contribution is too small to change the total form of the wave propagation, which should be close to the adiabatic one at all the temperatures since absorption is small. At the same time, discussing the elastic properties of the Jahn-Teller subsystem we can state that above 20 K its relaxation time is small enough and at the frequencies used in our experiment the isothermal regime is established (fast energy exchange with the lattice). At low temperatures the isothermal modulus usually has the temperature dependence as $1/T$. In our experiment this fact manifests itself in a certain softening of the dynamic modulus until $T\approx 18$K and a pronounced softening of the relaxed modulus at $T\lesssim 70$ when the temperature is reduced. To check the $1/T$ dependence of the unrelaxed modulus, in Fig. 6 we presented the data as functions of inverse temperature and noticed a well-defined straight line for the plot of $(C_R-C_0)/C_0$ at $T\lesssim 60$K. At $T\gtrsim 70$K we observed hardening (also when the temperature is reduced) of the dynamic modulus typical for the temperature

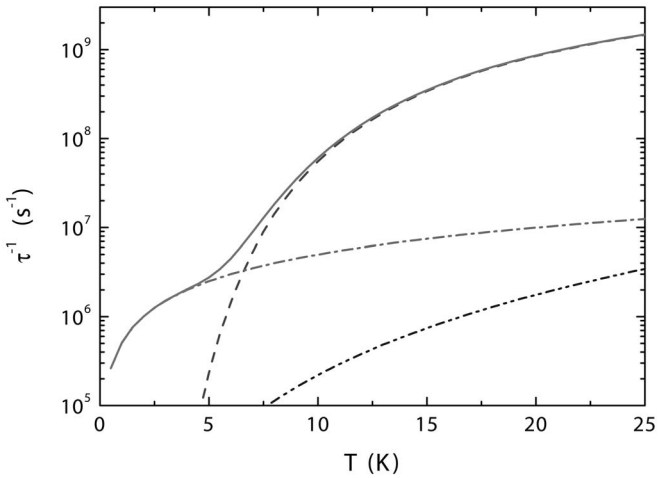

FIG. 7. Relaxation rate and its summands versus temperature calculated with the use of Eqs. (9)–(12). Solid curve for τ^{-1}, dashed curve for τ_T^{-1}, dashed-dotted curve for τ_t^{-1}, and dashed-dotted-dotted curve for τ_R^{-1}.

dependence of the second-order elastic constants in cubic materials.[23]

Another useful information, which helps to understand the temperature dependence of the relaxation time, can be obtained if we draw the dependences of different contributions given by Eqs. (10)–(12). The result is shown in Fig. 7. It becomes clear that the dominant mechanism of relaxation above 6 K is thermal activation over the potential barrier. At $T<6$K tunnelling accompanied by phonon emission becomes the dominant process of relaxation. The two-phonon process is small enough in comparison with other mechanisms at all investigated temperatures.

If we compare the dependence $\mathrm{Re}\,\Delta C/C_0$ with one obtained in $ZnSe:Ni^{2+}$, we should outline that the $ZnSe:Cr^{2+}$ crystal does not show such lattice instability. The reason for this fact we see in the difference of the ground terms of the impurities and, as a result, in different sets of the nonvanishing components of the deformation potential. We will discuss this problem in another paper since experiments done with the use of shear waves are required.

IV. CONCLUSION

Manifestation of the Jahn-Teller effect in ultrasonic experiment was discovered in one more crystal, namely, $ZnSe:Cr^{2+}$. The temperature dependence of the relaxation time was restored. Fitting of the dependence was done by means of three mechanisms of relaxation: thermal activation over the potential barrier, quantum tunnelling accompanying phonon emission, and two-phonon process. Data on the relaxation time made it possible to restore temperature dependences of the relaxed and unrelaxed moduli, to compare the results with ones obtained in $ZnSe:Ni^{2+}$ and analyze them regarding the lattice stability of the crystals.

Finally, it should be noted that in our paper it was shown that ultrasonic experiment reveals specific features of the lowest energy states that cannot be investigated by means of optic experiment.

ACKNOWLEDGMENTS

This work has been supported by the Russian Foundation for Basic Research (Grants Nos. 03-02-16246 and 04-02-96094-r2004 ural_a).

*Also at Russian State Vocational Pedagogial University, Ekaterinburg, Russia. Electronic address: gudkov@imp.uran.ru
†Electronic address: lonchakov@imp.uran.ru
‡Electronic address: visokolov@imp.uran.ru
§Electronic address: zhevstovskikh@imp.uran.ru

[1] T. V. Anil, C. S. Menon, K. S. Krishna, and K. P. Jayachandran, J. Phys. Chem. Solids **65**, 1053 (2004).
[2] C. Persson and A. Zunger, Phys. Rev. B **68**, 073205 (2003).
[3] K. A. Kikoin and V. N. Fleurov, *Transition Metal Impurities in Semiconductors: Electronic Structure and Physical Properties* (World Scientific, Singapore, 1994).
[4] G. Bevilacqua, L. Martinelli, and E. E. Vogel, Phys. Rev. B **66**, 155338 (2002).
[5] O. Mualin, E. E. Vogel, M. A. deOrue, L. Martinelli, G. Bevilacgua, and H.-J. Schulz, Phys. Rev. B **65**, 035211 (2001).
[6] H. Katayama-Yoshida and K. Sato, Physica B **327**, 337 (2003).
[7] E. Sorokin and I. T. Sorokina, Appl. Phys. Lett. **80**, 3289 (2002).
[8] G. A. Slack, Phys. Rev. B **6**, 3791 (1972).
[9] V. I. Sokolov and A. T. Lonchakov, JETP Lett. **73**, 708 (2001).
[10] V. I. Sokolov, S. F. Dubinin, S. G. Teploukhov, V. D. Parkhomenko, A. T. Lonchakov, V. V. Gudkov, A. V. Tkach, I. V. Zhevstovskikh, and N. B. Gruzdev, Solid State Commun. **129**, 507 (2004).
[11] V. V. Gudkov, A. T. Lonchakov, A. V. Tkach, I. V. Zhevstovskikh, V. I. Sokolov, and N. B. Gruzdev, J. Electron. Mater. **33**, 815 (2004).
[12] V. V. Gudkov, S. B. Petrov, A. T. Lonchakov, I. V. Zhevstovskikh, V. I. Sokolov, and N. B. Gruzdev, Low Temp. Phys. **30**, 912 (2004).
[13] T. Goto, Y. Nemoto, A. Ochiai, and T. Suzuki, Phys. Rev. B **59**, 269 (1999).
[14] J. M. Baranovski, J. M. Noras, and J. W. Allen, J. Phys. C **7**, 4529 (1974).
[15] M. D. Sturge, *Solid State Physics* (Academic, New York, London, 1967), Chap. The Jahn-Teller Effect in Solids, pp. 92–211.
[16] V. Gudkov, A. Lonchakov, V. Sokolov, I. Zhevstovskikh, and N. Gruzdev, Phys. Status Solidi B **242**, R30 (2005).
[17] T. L. Estle and W. C. Holton, Phys. Rev. **150**, 159 (1966).
[18] G. Bevilacqua, L. Martinelli, E. E. Vogel, and O. Mualin, Phys. Rev. B **70**, 075206 (2004).
[19] A. T. Lonchakov, V. I. Sokolov, and N. B. Gruzdev, Phys. Status Solidi C **1**, 2967 (2004).
[20] V. V. Gudkov and J. D. Gavenda, *Magnetoacoustic Polarization Phenomena in Solids* (Springer-Verlag, New York, Berlin, Heidelberg, 2000).
[21] M. Pomerantz, Proc. IEEE **53**, 1438 (1965).
[22] W. Luo, S. Ismail-Beigi, M. L. Cohen, and S. G. Louie, Phys. Rev. B **66**, 195215 (2002).
[23] J. A. Garber and A. V. Granato, Phys. Rev. B **11**, 3990 (1975).